bc diquark pair production in high energy proton-proton collisions

Anton Trunin[*]

Bogoliubov Laboratory of Theoretical Physics, Joint Institute for Nuclear Research,
Joliot-Curie Street 6, 141980 Dubna, Russia
and Samara State Aerospace University, Moskovskoye Shosse 34, 443086 Samara, Russia
(Received 9 March 2016; published 24 June 2016)

The cross section of the double heavy diquark pair production process $pp \to (bc) + (\bar{b}\,\bar{c}) + X$ is calculated in the leading order of the gluonic fusion channel, with all four possible color and spin combinations—$[^1S_0]_{\bar{3}}$, $[^1S_0]_6$, $[^3S_1]_{\bar{3}}$, and $[^3S_1]_6$ for each of the two final diquarks—taken into account. Several sources of relativistic corrections to the cross section are handled in the framework of the relativistic quark model. Perturbative $\mathcal{O}(v^2)$ corrections originating from the production amplitude expansions in heavy quark relative velocity v depend on the color and spin states of the final particles, but can be generally considered as unimportant, giving maximally 12% improvement in numerically significant cases. Modifications of the quark-quark and antiquark-antiquark bound state wave functions caused by the appropriate generalization of the Breit interaction potential have a rather severe impact on the cross section, suppressing it almost 3 times. Under the assumption of antitriplets' and sextuplets' nonperturbative parameters having the same order of magnitude, it is shown that the color-sextet mechanism strongly dominates pair diquark production in both nonrelativistic and relativistic approximations.

I. INTRODUCTION

At the moment, contrary to the broadly studied charmonium and single heavy baryon families, there are no concrete experimental results on baryons containing two heavy *b* or *c* quarks. Initially, their first experimental observation was reported by the SELEX Collaboration more than ten years ago, but it is still not confirmed in any subsequent experimental study followed since then [1,2]. Theoretical investigation of the double heavy baryons, motivated by the uncertain experimental situation as well as by unique properties and the wide range of physics associated with such systems, represents an actively developing field [3–11]. The double heavy baryons provide a remarkable opportunity to test quantum chromodynamics (QCD) and several effective theories based on it in both hard and low-energy regions. The heavy quarks Q and Q' within the baryon $(QQ'q)$ are predicted to form a heavy diquark—a compact quark-quark bound state (QQ') in an antitriplet or, alternatively, a sextuplet color state [12,13]. With respect to the picture of strong interaction, a heavy diquark in an antitriplet color state is equal to an antiquark in a heavy-light meson: the smallness of the diquark radius $r_{QQ'} \ll \Lambda_{\text{QCD}}$ allows us to consider it as an almost static and pointlike source of gluonic field, so that the dynamics of the light quark q in both types of hadrons is expected to be quite similar. Therefore, the double heavy baryons combine the aspects of both heavy-heavy and heavy-light quark bound states and can serve as an independent test object for the

respective models and theoretical constructions, like NRQCD [14] and HQET [15]. Moreover, there is a close connection between the double heavy baryons and even more unusual diquark bound states, such as double heavy tetraquarks [10,16]. The latter can be considered as possible candidates for some states from the broad list of exotic "XYZ" resonances discovered during the last several years [17].

According to the quark-diquark model, the production of a double heavy baryon is divided into two stages. In the first step, which is described by perturbative QCD, the creation of two quark-antiquark pairs $Q\bar{Q}$ and $Q'\bar{Q}'$ takes place. In the second step, the created quarks and antiquarks rearrange to form the bound state of the heavy diquark (QQ') or $(\bar{Q}\bar{Q}')$ with its subsequent hadronization to the observable double heavy baryon. The transition of the heavy diquark into the baryon is generally covered by the appropriate fragmentation functions $D_{(QQ')\to(QQ'q)}(z)$ [3,18]. Nevertheless, taking into account the several-order-of-magnitude difference between heavy diquark and light quark masses, the diquark can be assumed to carry almost all of the final baryon momentum, so that the corresponding fragmentation function approximates to $D_{(QQ')\to(QQ'q)}(z) = \delta(1-z)P_{(QQ')\to(QQ'q)}$ [13]. The applicability of such approximation was confirmed by direct calculations in Ref. [19]. Although the heavy diquark (QQ') bounds the light quark q very easily, there is also a possibility for the diquark dissociation events decreasing the total transition probability $P_{(QQ')\to(QQ'q)} < 1$. Therefore, cross sections of double heavy diquarks represent an upper bound for the yield of double heavy

---

[*]amtrnn@gmail.com

114029-1

baryons in the same reaction, summed over light quark flavors and over all possible baryon spin states. The nonperturbative stage of heavy baryon production can be described by the appropriate matrix elements of NRQCD, for which, due to the lack of experimental data, the potential model predictions for $|\Psi_{(QQ')}(0)|^2$ are used.

The pair production of double heavy baryons in e^+e^- annihilation and pp collisions was studied in Refs. [20–22]. In all these studies, however, only the case of (anti)triplet color states of the two final diquarks has been considered. As was already mentioned, the heavy diquark can be produced either in an antitriplet or in a sextuplet color configuration, representing a close analogy to the color-singlet and color-octet mechanisms of heavy quarkonium production [14]. Both the octet and sextuplet cases require an additional gluon to be emitted in the nonperturbative part of the process, what generally $\mathcal{O}(v^2)$-suppresses the appropriate matrix elements, if the required emission is attributed to the heavy quark of relative velocity v. Nevertheless, in the case of a double heavy baryon, the final state also contains a light quark, which produces a gluon easily, so that the different power-counting rules can be applied, and both antitriplet and sextuplet matrix elements turn out to be of the same order [23]. Under this assumption, the sextuplet mechanism was shown to be equally or even more important than the conventional antitriplet channel for various high-energy processes of double heavy baryon production [19,23–28].

This paper is focused on the pair production of double heavy (bc) diquarks in proton-proton collisions, with all four possible color and spin combinations $[^1S_0]_{\bar{3}}$, $[^1S_0]_6$, $[^3S_1]_{\bar{3}}$, $[^3S_1]_6$ for each of the two final diquarks taken into account. The calculation technique is based on the notion of the relativistic quark model with the elements of the quasipotential approach [29], which was first applied to the problems of pair charmonium production in Ref. [30]. Our consideration is limited by the gluon fusion processes, for which the initial state of proton collision is approximated by the gluonic pair gg. The alternative possibilities, such as the so-called "intrinsic charm" processes with initial states gc or cc, were studied in Refs. [5,24] in connection with single Ξ_{cc} baryon production. There it was shown that the intrinsic charm mechanism is crucial under SELEX kinematical conditions, while its contributions are much less important in the Tevatron and LHC cases. The paper is organized as follows: In Sec. II the general formalism of the applied approach is briefly described. The exact expression for the relativistic production amplitude is given in the leading order in the strong coupling constant, and general formulas for the cross sections of pair diquark production are presented, taking into account second-order relativistic corrections in v. Section III contains numerical details of the model and results for the cross

sections calculated at the LHC c.m. energies $\sqrt{S} = 7$ and 14 TeV in nonrelativistic and relativistic approximations. The role of sextuplet contributions is discussed, and several sources of relativistic corrections are analyzed. The Appendix delivers a short note on the structure of electronic Supplemental Material [31] to the paper.

II. GENERAL FORMALISM

The cross section of pair double heavy diquark production in proton-proton collisions can be presented in the following form, corresponding to the collinear approximation for colliding protons [22,32]:

$$
d\sigma[p + p \to D_{bc} + \bar{D}_{\bar{b}\bar{c}} + X]
$$
$$
= \int dx_1 dx_2 f_{g/p}(x_1, \mu) f_{g/p}(x_2, \mu) d\sigma[gg \to D_{bc} + \bar{D}_{\bar{b}\bar{c}}],
$$

(1)

where $f_{g/p}(x, \mu)$ is the partonic distribution function for the gluon in a proton, $x_{1,2}$ are the longitudinal momentum fractions of gluons, and μ is the factorization scale. Neglecting the proton mass and taking the c.m. reference frame of the initial protons with the beam along the z axis, we can present the gluon on-mass-shell momenta as $k_{1,2} = x_{1,2} \frac{\sqrt{S}}{2}(1, 0, 0, \pm 1)$. At the high center-of-mass energy $\sqrt{S}$ in proton-proton collisions, the main contribution to the cross section (1) is expected to come from the gluon fusion process $gg \to D_{bc} + \bar{D}_{\bar{b}\bar{c}}$.

Taking into account two spin and color states for each of the final diquarks, there are 16 different subprocesses contributing to the pair diquark production. Only 10 of them are independent, while cross sections for the rest can be obtained from the respective symmetry relations. Nevertheless, contributions from all 16 processes eventually have to be summed up in order to obtain an estimate for pair double heavy baryon production. In the quasipotential approach, the production amplitude for the gluonic subprocess $gg \to D_{bc} + \bar{D}_{\bar{b}\bar{c}}$ can be expressed as a convolution of the perturbative production amplitude of (bc) and $(\bar{b}\bar{c})$ (anti)quark pairs $\mathcal{T}(p_1, p_2; q_1, q_2)$ and the quasipotential wave functions of the final diquarks $\Psi_{(bc)}(p, P)$ and $\Psi_{(\bar{b}\bar{c})}(q, Q)$ [30]:

$$
\mathcal{M}[gg \to D_{bc} + \bar{D}_{\bar{b}\bar{c}}](k_1, k_2, P, Q)
$$
$$
= \int \frac{d\mathbf{p}}{(2\pi)^3} \int \frac{d\mathbf{q}}{(2\pi)^3} \bar{\Psi}_{(bc)}(p, P) \bar{\Psi}_{(\bar{b}\bar{c})}(q, Q)
$$
$$
\otimes \mathcal{T}(p_1, p_2; q_1, q_2),
$$

(2)

where $p_{1,2}$ are four-momenta of c and b quarks, and $q_{1,2}$ are the appropriate four-momenta for $\bar{c}$ and $\bar{b}$ antiquarks. They are defined in terms of total momenta $P(Q)$ and relative momenta $p(q)$ as follows:
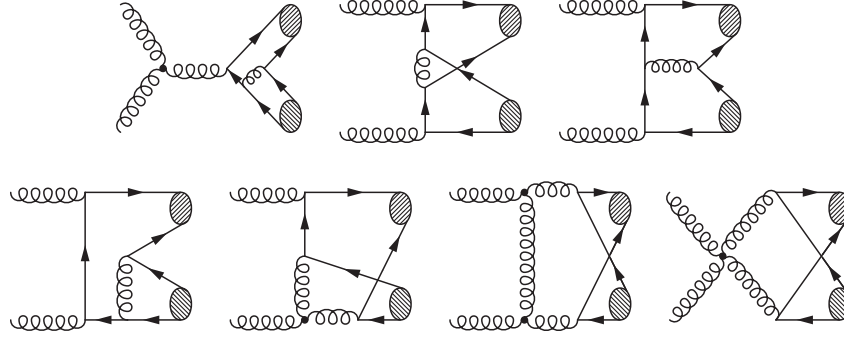
FIG. 1. The leading-order diagrams contributing to $gg \to D_{bc} + \bar{D}_{\bar{b}\bar{c}}$. The others can be obtained by reversing the quark lines or interchanging the initial gluons.
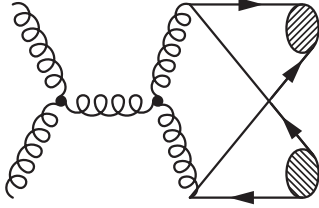

FIG. 2. One additional leading-order diagram contributing only to the subprocesses with color states $\bar{3} + \bar{6}$ or $6 + 3$ of the final diquark pair $D_{bc} + \bar{D}_{\bar{b}\bar{c}}$.

$$
\begin{aligned}
p_{1,2} &= \eta_{1,2} P \pm p, \qquad (pP) = 0, \\
q_{1,2} &= \rho_{1,2} Q \pm q, \qquad (qQ) = 0, \\
\eta_{1,2} &= \frac{M_{bc}^2 \pm m_c^2 \mp m_b^2}{2M_{bc}^2}, \qquad \rho_{1,2} = \frac{M_{\bar{b}\bar{c}}^2 \pm m_c^2 \mp m_b^2}{2M_{\bar{b}\bar{c}}^2},
\end{aligned}
\tag{3}
$$

where $m_{c,b}$ are quark masses, $M_{bc} = M_{D_{bc}}$ and $M_{\bar{b}\bar{c}} = M_{\bar{D}_{\bar{b}\bar{c}}}$ are diquark masses, $p = L_P(0, \mathbf{p})$ and $q = L_Q(0, \mathbf{q})$ are the relative four-momenta obtained by the Lorentz transformation of the four-vectors $(0, \mathbf{p})$ and $(0, \mathbf{q})$ to the reference frames moving with the four-momenta P and Q of the final diquarks D_{bc} and $\bar{D}_{\bar{b}\bar{c}}$, respectively. The integration in Eq. (2) is performed over the relative three-momenta of quarks and antiquarks in the final state.

In the leading order in the strong coupling constant α_s, there are 36 Feynman diagrams describing the process $gg \to D_{bc} + \bar{D}_{\bar{b}\bar{c}}$, which are presented in Figs. 1 and 2. The single diagram from Fig. 2 produces a nonzero contribution only if the resulting pair $D_{bc} + \bar{D}_{\bar{b}\bar{c}}$ contains diquarks with the color combination $\bar{3} + \bar{6}$ or $6 + 3$, and it still always vanishes for the final state consisting of two scalar diquarks $SD_{bc} + S\bar{D}_{\bar{b}\bar{c}}$. Due to the large volume of calculations, the package FeynArts [33] for Mathematica was used to obtain analytical expressions for all diagrams, and their traces were subsequently calculated with Form [34]. Then the leading-order production amplitude (2) reads

$$
\begin{aligned}
\mathcal{M}[gg \to D_{bc} + \bar{D}_{\bar{b}\bar{c}}](k_1, k_2, P, Q) &= \sqrt{M_{bc} M_{\bar{b}\bar{c}}} \, \pi^2 \alpha_s^2 \int \frac{d\mathbf{p}}{(2\pi)^3} \int \frac{d\mathbf{q}}{(2\pi)^3} \, \mathrm{Tr}\,\mathfrak{M}, \\
\mathfrak{M} &= \bar{\Psi}_{P,p}^{bc} \gamma_\beta \bar{\Psi}_{Q,q}^{cb} \gamma_\omega \Gamma_1^{\beta\omega} + \bar{\Psi}_{P,-p}^{cb} \gamma_\beta \Gamma_2^{\beta\omega\theta} \gamma_\omega \bar{\Psi}_{Q,-q}^{bc} \gamma_\theta + \bar{\Psi}_{P,p}^{bc} \gamma_\beta \Gamma_3^{\beta\omega\theta} \gamma_\omega \bar{\Psi}_{Q,q}^{cb} \gamma_\theta \\
&\quad + \bar{\Psi}_{P,p}^{bc} \hat{\varepsilon}_1 \frac{m_c - \hat{k}_1 + \hat{p}_1}{(k_1 - p_1)^2 - m_c^2} \gamma_\beta (\bar{\Psi}_{Q,q}^{cb} \gamma_\omega \Gamma_4^{\beta\omega} + \Gamma_5^{\beta\omega} \bar{\Psi}_{Q,q}^{cb} \gamma_\omega) \\
&\quad + \bar{\Psi}_{P,-p}^{cb} \hat{\varepsilon}_1 \frac{m_b - \hat{k}_1 + \hat{p}_2}{(k_1 - p_2)^2 - m_b^2} \gamma_\beta (\bar{\Psi}_{Q,-q}^{bc} \gamma_\omega \Gamma_6^{\beta\omega} + \Gamma_7^{\beta\omega} \bar{\Psi}_{Q,-q}^{bc} \gamma_\omega) \\
&\quad + \bar{\Psi}_{P,p}^{bc} \hat{\varepsilon}_2 \frac{m_c - \hat{k}_2 + \hat{p}_1}{(k_2 - p_1)^2 - m_c^2} \gamma_\beta \Gamma_8^{\beta\omega} \bar{\Psi}_{Q,q}^{cb} \gamma_\omega + \bar{\Psi}_{P,-p}^{cb} \hat{\varepsilon}_2 \frac{m_b - \hat{k}_2 + \hat{p}_2}{(k_2 - p_2)^2 - m_b^2} \gamma_\beta \Gamma_9^{\beta\omega} \bar{\Psi}_{Q,-q}^{bc} \gamma_\omega \\
&\quad + \bar{\Psi}_{P,-p}^{cb} \gamma_\beta \frac{m_b + \hat{k}_1 - \hat{q}_2}{(k_1 - q_2)^2 - m_b^2} \hat{\varepsilon}_1 \bar{\Psi}_{Q,-q}^{bc} \gamma_\omega \Gamma_{10}^{\beta\omega} + \bar{\Psi}_{P,p}^{bc} \gamma_\beta \frac{m_c + \hat{k}_1 - \hat{q}_1}{(k_1 - q_1)^2 - m_c^2} \hat{\varepsilon}_1 \bar{\Psi}_{Q,q}^{cb} \gamma_\omega \Gamma_{11}^{\beta\omega},
\end{aligned}
\tag{4}
$$

where $\varepsilon_{1,2}$ are polarization vectors of the initial gluons, the hat symbol means contraction of the four-vector with the Dirac gamma matrices, and vertex functions Γ_i were introduced to make the entry of the amplitude (4) more compact. The normalization factors $\sqrt{2M_{bc}}$ and $\sqrt{2M_{\bar{b}\bar{c}}}$ of the quasipotential bound-state wave functions were explicitly extracted in (4).

The formation of diquark states from (anti)quark pairs, which corresponds to the first stage of double heavy baryon formation, is determined in the quark model by the quasipotential wave functions $\Psi_{bc}(p,P)$ and $\Psi_{\bar{b}\bar{c}}(q,Q)$. These wave functions are calculated initially in the diquark rest frame and then transformed to the reference frames moving with the four-momenta P and Q. The law of such transformations was derived in the Bethe-Salpeter approach in Ref. [35] and in the quasipotential method in Ref. [36]. The latter gives the following expressions for the relativistic wave functions [21]:

$$\bar{\Psi}^{bc}_{P,p} = \frac{\bar{\Psi}^0_{bc}(\mathbf{p})}{\sqrt{\frac{e_c(p)}{m_c}\frac{e_c(p)+m_c}{2m_c}\frac{e_b(p)}{m_b}\frac{e_b(p)+m_b}{2m_b}}}\left[\frac{\hat{v}_1-1}{2} + \hat{v}_1\frac{\mathbf{p}^2}{2m_b(e_b(p)+m_b)} - \frac{\hat{p}}{2m_b}\right]$$

$$\times \Sigma^P(1+\hat{v}_1)\left[\frac{\hat{v}_1+1}{2} + \hat{v}_1\frac{\mathbf{p}^2}{2m_c(e_c(p)+m_c)} + \frac{\hat{p}}{2m_c}\right],$$

$$\bar{\Psi}^{cb}_{Q,q} = \frac{\bar{\Psi}^0_{\bar{b}\bar{c}}(\mathbf{q})}{\sqrt{\frac{e_c(q)}{m_c}\frac{e_c(q)+m_c}{2m_c}\frac{e_b(q)}{m_b}\frac{e_b(q)+m_b}{2m_b}}}\left[\frac{\hat{v}_2-1}{2} + \hat{v}_2\frac{\mathbf{q}^2}{2m_c(e_c(q)+m_c)} + \frac{\hat{q}}{2m_c}\right]$$

$$\times \Sigma^Q(1+\hat{v}_2)\left[\frac{\hat{v}_2+1}{2} + \hat{v}_2\frac{\mathbf{q}^2}{2m_b(e_b(q)+m_b)} - \frac{\hat{q}}{2m_b}\right], \tag{5}$$

where $e_{c,b}(p) = \sqrt{p^2 + m_{c,b}^2}$, $v_1 = P/M_{bc}$, $v_2 = Q/M_{\bar{b}\bar{c}}$, and $\Sigma^{P,Q}$ is equal to γ_5 and $\hat{\varepsilon}_{P,Q}$ for scalar (S) and axial-vector (AV) diquarks, respectively. The polarization vectors $\varepsilon_{P,Q}$ of the axial-vector diquarks fulfill the relations $(\varepsilon_P P) = 0$ and $(\varepsilon_Q Q) = 0$. The quasipotential wave functions (5) include (anti)quark pair-projection operators for the given spin states $\bar{u}_i(0)\bar{u}_j(0) = [C\hat{\varepsilon}(\gamma_5)(1+\gamma_0)]_{ij}/2\sqrt{2}$

and $v_i(0)v_j(0) = [(1-\gamma_0)\hat{\varepsilon}(\gamma_5)C]_{ij}/2\sqrt{2}$, where C is the charge conjugation matrix. Note that the order of the upper indices b and c in the left-hand side of the definitions in Eq. (5) is important, so that their permutation leads to the proper replacements $m_c \leftrightarrow m_b$ applied to the right-hand side of Eq. (5).

Leading-order vertex functions Γ_i in (4) have the following explicit form:

$$\Gamma_1^{\beta\omega} = \mathcal{K}_1 D_\mu{}^\beta(p_1+q_1)D_\nu{}^\omega(p_2+q_2)((2-\kappa_c)(\varepsilon_1^\nu\varepsilon_2^\mu + \kappa_c\varepsilon_1^\mu\varepsilon_2^\nu) - (1+\kappa_c)g^{\mu\nu}(\varepsilon_1\varepsilon_2)$$

$$- iD_{\lambda\kappa}(k_1-p_1-q_1)\mathfrak{C}_1^{\lambda\mu}(p_1+q_1)\mathfrak{C}_2^{\kappa\nu}(p_2+q_2) - i\kappa_c D_{\kappa\lambda}(k_1-p_2-q_2)\mathfrak{C}_1^{\kappa\nu}(p_2+q_2)\mathfrak{C}_2^{\lambda\mu}(p_1+q_1)$$

$$+ i(1-\kappa_c)D_{\kappa\theta}(k_1+k_2)\mathfrak{C}_1^\kappa(-k_2)\mathfrak{Q}^{\mu\theta\nu}(k_1+k_2,p_2+q_2)),$$

$$\Gamma_2^{\beta\omega\theta} = \kappa_s\mathcal{K}_2\mathfrak{C}_2^\mu(-k_1)D_\mu{}^\beta(k_1+k_2)D^{\theta\omega}(p_1+q_1)\frac{m_b-\hat{p}_1-\hat{q}_1-\hat{q}_2}{(p_1+q_1+q_2)^2-m_b^2} + \kappa_s\mathcal{K}_{12}\varepsilon_2^\omega\mathfrak{C}_1^{\mu\nu}(p_1+q_1)$$

$$\times D_\mu{}^\beta(k_1-p_1-q_1)D_\nu{}^\theta(p_1+q_1)\frac{m_b+k_2-q_2}{(k_2-q_2)^2-m_b^2} + \kappa_s\Delta_c D^{\theta\beta}(p_1+q_1)\frac{m_b+\hat{p}_1+\hat{p}_2+\hat{q}_1}{(p_1+p_2+q_1)^2-m_b^2}$$

$$\times \left(\kappa_c\mathcal{K}_2\mathfrak{C}_1^\mu(-k_2)D_\mu{}^\omega(k_1+k_2) + \mathcal{K}_9\varepsilon_1^\omega\hat{\varepsilon}_2\frac{m_b+\hat{k}_1-\hat{q}_2}{(k_1-q_2)^2-m_b^2} + \mathcal{K}_7\varepsilon_2^\omega\hat{\varepsilon}_1\frac{m_b+\hat{k}_2-\hat{q}_2}{(k_2-q_2)^2-m_b^2}\right),$$

$$\Gamma_4^{\beta\omega} = \mathcal{K}_3 D^{\beta\omega}(k_1-p_1-q_1)\frac{m_b+\hat{k}_2-\hat{p}_2}{(k_2-p_2)^2-m_b^2}\hat{\varepsilon}_2 - \mathcal{K}_4\varepsilon_2^\omega D^{\beta\mu}(k_1-p_1-q_1)\frac{m_b-\hat{k}_2+\hat{q}_2}{(k_2-q_2)^2-m_b^2}\gamma_\mu$$

$$- \mathcal{K}_5\mathfrak{C}_2^{\mu\nu}(p_2+q_2)D_\mu{}^\beta(k_1-p_1-q_1)D_\nu{}^\omega(p_2+q_2),$$

$$\Gamma_5^{\beta\omega} = \mathcal{K}_6 D^{\beta\omega}(p_2+q_2)\frac{m_c+\hat{k}_2-\hat{q}_1}{(k_2-q_1)^2-m_c^2}\hat{\varepsilon}_2 + \mathcal{K}_7\varepsilon_2^\beta D_\mu{}^\omega(p_2+q_2)\frac{m_c-\hat{p}_2-\hat{q}_1-\hat{q}_2}{(p_2+q_1+q_2)^2-m_c^2}\gamma_\mu,$$

$$\Gamma_8^{\beta\omega} = \mathcal{K}_8 D^{\beta\omega}(p_2+q_2)\frac{m_c+\hat{k}_1-\hat{q}_1}{(k_1-q_1)^2-m_c^2}\hat{\varepsilon}_1 + \mathcal{K}_9\varepsilon_1^{\beta}D_\mu^{\ \omega}(p_2+q_2)\frac{m_c-\hat{p}_2-\hat{q}_1-\hat{q}_2}{(p_2+q_1+q_2)^2-m_c^2}\gamma_\mu$$
$$-\mathcal{K}_{10}\mathfrak{E}_1^{\mu\nu}(p_2+q_2)D_\mu^{\ \beta}(k_1-p_2-q_2)D_\nu^{\ \omega}(p_2+q_2),$$

$$\Gamma_{10}^{\beta\omega} = \kappa_s\mathcal{K}_{11}D^{\beta\omega}(k_1-p_2-q_2)\frac{m_c+\hat{k}_2-\hat{p}_1}{(k_2-p_1)^2-m_c^2}\hat{\varepsilon}_2 + \kappa_s\Delta_c\mathcal{K}_3\varepsilon_2^{\omega}D^{\beta\mu}(k_1-p_2-q_2)\frac{m_c-\hat{k}_2+\hat{q}_1}{(k_2-q_1)^2-m_c^2}\gamma_\mu$$
$$+\kappa_s\mathcal{K}_{13}\mathfrak{E}_2^{\mu\nu}(p_1+q_1)D_\mu^{\ \beta}(k_1-p_2-q_2)D_\nu^{\ \omega}(p_1+q_1), \tag{6}$$

where the constant κ_s equals $+1$ in the case of the equal spin states of the final diquark pair $S(AV)+S(AV)$ and -1 for the other two possibilities $S(AV)+AV(S)$. Analogously, $\kappa_c=+1$ for $\bar{3}(6)+3(\bar{6})$, $\kappa_c=-1$ for $\bar{3}(6)+\bar{6}(3)$, and the values of $\Delta_c=1/2,2,1$ correspond to the final color states $6+3$, $\bar{3}+\bar{6}$, and $\bar{3}(6)+3(\bar{6})$, respectively. The following tensors are introduced:

$$\mathfrak{L}^{\mu\nu\omega}(x,y) = g^{\mu\nu}(y^\omega-2x^\omega) - g^{\omega\mu}(2y^\nu-x^\nu) + g^{\omega\nu}(x^\mu+y^\mu),$$
$$\mathfrak{E}_{1,2}^{\mu\nu}(x) = \varepsilon_{1,2}^\omega L^{\mu\nu}_{\ \ \omega}(x,k_{1,2}), \qquad \mathfrak{E}_{1,2}^\mu(x) = \varepsilon_{2,1}^\nu \mathfrak{E}_{1,2}^{\mu\nu}(x), \tag{7}$$

and $D_{\mu\nu}(k)$ is the gluon propagator, which is subsequently taken in the Feynman gauge $D_F^{\mu\nu}(k)=-ig^{\mu\nu}/k^2$. The additional vertex functions Γ_i can be found by the simultaneous replacements $m_c \leftrightarrow m_b$, $p_1 \leftrightarrow p_2$, and $q_1 \leftrightarrow q_2$ in Eq. (6):

$$\Gamma_3^{\beta\omega\theta} = \kappa_s\kappa_c\Gamma_2^{\beta\omega\theta}\Big|_{\substack{m_b\rightleftarrows m_c\\p_1\rightleftarrows p_2\\q_1\rightleftarrows q_2}}, \quad \Gamma_6^{\beta\omega}=\kappa_s\kappa_c\Gamma_4^{\beta\omega}\Big|_{\substack{m_b\rightleftarrows m_c\\p_1\rightleftarrows p_2\\q_1\rightleftarrows q_2}}, \quad \Gamma_7^{\beta\omega}=\kappa_s\kappa_c\Gamma_5^{\beta\omega}\Big|_{\substack{m_b\rightleftarrows m_c\\p_1\rightleftarrows p_2\\q_1\rightleftarrows q_2}}, \quad \Gamma_9^{\beta\omega}=\kappa_s\kappa_c\Gamma_8^{\beta\omega}\Big|_{\substack{m_b\rightleftarrows m_c\\p_1\rightleftarrows p_2\\q_1\rightleftarrows q_2}}, \quad \Gamma_{11}^{\beta\omega}=\kappa_s\kappa_c\Gamma_{10}^{\beta\omega}\Big|_{\substack{m_b\rightleftarrows m_c\\p_1\rightleftarrows p_2\\q_1\rightleftarrows q_2}}.$$
$$\tag{8}$$

The 36 leading-order Feynman diagrams summed with the antisymmetric color functions $\epsilon^{c_1c_2A}/\sqrt{2}$ ($c_i,A=1,2,3$) of (anti)triplet diquarks and/or with the partially symmetric functions $d^{c_1c_2A}/\sqrt{2}$ ($A=1,...,6$) of (anti)sextuplets lead to the nontrivial color structure of the production amplitude, which manifests itself through the color factors $\mathcal{K}_i$ in (6). For the $\bar{3}+3$ final state, we have[1]

$$\mathcal{K}_1=-2\mathcal{C}_0-3\mathcal{C}_1+6\mathcal{C}_2, \qquad \mathcal{K}_2=\frac{4}{3}\mathcal{C}_1, \qquad \mathcal{K}_3=\frac{2i}{3}(\mathcal{C}_0+2\mathcal{C}_1-4\mathcal{C}_2), \qquad \mathcal{K}_4=\frac{i}{3}(\mathcal{C}_0-\mathcal{C}_1-\mathcal{C}_2),$$

$$\mathcal{K}_5=\mathcal{C}_0+\mathcal{C}_1-3\mathcal{C}_2, \qquad \mathcal{K}_6=-\frac{i}{3}(\mathcal{C}_0+3\mathcal{C}_1-5\mathcal{C}_2), \qquad \mathcal{K}_7=\frac{2i}{3}(\mathcal{C}_0-2\mathcal{C}_2), \qquad \mathcal{K}_8=-\frac{i}{3}(\mathcal{C}_0+2\mathcal{C}_1-5\mathcal{C}_2),$$

$$\mathcal{K}_9=\frac{2i}{3}(\mathcal{C}_0+2\mathcal{C}_1-2\mathcal{C}_2), \qquad \mathcal{K}_{10}=\mathcal{C}_0+2\mathcal{C}_1-3\mathcal{C}_2, \qquad \mathcal{K}_{11}=-\frac{i}{3}(\mathcal{C}_0+2\mathcal{C}_1-\mathcal{C}_2), \qquad \mathcal{K}_{12}=\mathcal{K}_5,$$

$$\mathcal{K}_{13}=\mathcal{K}_{10}, \qquad \mathcal{C}_0=\delta^{g_1g_2}\delta_{AB}, \qquad \mathcal{C}_1=if^{g_1g_2a}(T^a)_{BA}, \qquad \mathcal{C}_2=(T^{g_1}T^{g_2})_{BA}. \tag{9}$$

For $\bar{3}+\bar{6}$,

$$\mathcal{K}_1=\mathcal{C}_0, \qquad \mathcal{K}_2=-\frac{2}{3}\mathcal{C}_0, \qquad \mathcal{K}_3=\frac{2i}{3}\mathcal{C}_1, \qquad \mathcal{K}_4=\frac{i}{3}(\mathcal{C}_1-3\mathcal{C}_2), \qquad \mathcal{K}_5=\mathcal{C}_1-\mathcal{C}_2, \qquad \mathcal{K}_6=-\frac{i}{3}(3\mathcal{C}_1-\mathcal{C}_2),$$

$$\mathcal{K}_7=-\frac{2i}{3}\mathcal{C}_2, \qquad \mathcal{K}_8=-\frac{i}{3}(\mathcal{C}_0-3\mathcal{C}_1-\mathcal{C}_2), \qquad \mathcal{K}_9=\frac{2i}{3}(\mathcal{C}_0-\mathcal{C}_2), \qquad \mathcal{K}_{10}=\mathcal{C}_0-\mathcal{C}_1-\mathcal{C}_2,$$

$$\mathcal{K}_{11}=-\frac{i}{3}(3\mathcal{C}_0-\mathcal{C}_1-3\mathcal{C}_2), \qquad \mathcal{K}_{12}=-\mathcal{C}_1-\mathcal{C}_2, \qquad \mathcal{K}_{13}=\mathcal{C}_0+\mathcal{C}_1-\mathcal{C}_2. \tag{10}$$

For $6+3$,

---

[1]The author is grateful to S. P. Baranov for pointing out that the color structure of the amplitude can be additionally simplified in this case.

$$\mathcal{K}_1 = -\mathcal{C}_0, \quad \mathcal{K}_2 = \frac{4}{3}\mathcal{C}_0, \quad \mathcal{K}_3 = -\frac{4i}{3}\mathcal{C}_1, \quad \mathcal{K}_4 = \frac{i}{3}(\mathcal{C}_1 + 3\mathcal{C}_2), \quad \mathcal{K}_5 = -\mathcal{C}_1 + \mathcal{C}_2, \quad \mathcal{K}_6 = \frac{i}{3}(3\mathcal{C}_1 + \mathcal{C}_2),$$

$$\mathcal{K}_7 = \frac{4i}{3}\mathcal{C}_2, \quad \mathcal{K}_8 = -\frac{i}{3}(\mathcal{C}_0 + 3\mathcal{C}_1 - \mathcal{C}_2), \quad \mathcal{K}_9 = -\frac{4i}{3}(\mathcal{C}_0 - \mathcal{C}_2), \quad \mathcal{K}_{10} = -\mathcal{C}_0 + \mathcal{C}_1 + \mathcal{C}_2,$$

$$\mathcal{K}_{11} = \frac{i}{3}(3\mathcal{C}_0 + \mathcal{C}_1 - 3\mathcal{C}_2), \quad \mathcal{K}_{12} = \mathcal{C}_1 + \mathcal{C}_2, \quad \mathcal{K}_{13} = -\mathcal{C}_0 - \mathcal{C}_1 + \mathcal{C}_2. \tag{11}$$

And finally, for $6 + \bar{6}$,

$$\mathcal{K}_1 = -\mathcal{C}_0 - 2\mathcal{C}_1 + 2\mathcal{C}_2, \quad \mathcal{K}_2 = \frac{2}{3}\mathcal{C}_0, \quad \mathcal{K}_3 = \frac{2i}{3}\mathcal{C}_1, \quad \mathcal{K}_4 = \frac{i}{3}(\mathcal{C}_1 - 3\mathcal{C}_2), \quad \mathcal{K}_5 = \mathcal{C}_1 - \mathcal{C}_2,$$

$$\mathcal{K}_6 = -\frac{i}{3}(3\mathcal{C}_1 - \mathcal{C}_2), \quad \mathcal{K}_7 = -\frac{2i}{3}\mathcal{C}_2, \quad \mathcal{K}_8 = -\frac{i}{3}(\mathcal{C}_0 + 3\mathcal{C}_1 - \mathcal{C}_2), \quad \mathcal{K}_9 = \frac{2i}{3}(\mathcal{C}_0 - \mathcal{C}_2),$$

$$\mathcal{K}_{10} = \mathcal{C}_0 + \mathcal{C}_1 - \mathcal{C}_2, \quad \mathcal{K}_{11} = -\frac{i}{3}(3\mathcal{C}_0 + \mathcal{C}_1 - 3\mathcal{C}_2), \quad \mathcal{K}_{12} = \mathcal{K}_5, \quad \mathcal{K}_{13} = \mathcal{K}_{10}. \tag{12}$$

The coefficients $\mathcal{C}_i$ are written explicitly in Eq. (9) for the $\bar{3} + 3$ final color state, where f^{ijk} and T^a are $SU(3)$ structure constants and fundamental representation generators; $g_{1,2} = 1, \ldots, 8$ are color indices of initial gluons; and A and B are color indices of the diquarks D_{bc} and $\bar{D}_{\bar{b}\bar{c}}$, respectively. Note that the color factors of Ref. [22] agree with Eq. (9) after the equality $\mathcal{C}_3 = f^{g_1 ca} f^{g_2 cb}(T^a T^b)_{BA} = \mathcal{C}_0/4 + 3\mathcal{C}_2/2$ is applied. For all other color combinations, the following general form is valid:

$$\mathcal{C}_0 = i f^{g_1 g_2 a}(T^a)_{c_1 c_3} c_f^{c_1 c_2 A} c_f^{c_3 c_2 B},$$

$$\mathcal{C}_1 = (T^{g_1})_{c_1 c_3}(T^{g_2})_{c_2 c_4} c_f^{c_1 c_2 A} c_f^{c_3 c_4 B},$$

$$\mathcal{C}_2 = (T^{g_1} T^{g_2})_{c_1 c_3} c_f^{c_1 c_2 A} c_f^{c_3 c_2 B}, \tag{13}$$

where c_f stands for the corresponding color wave function ϵ or d.

The production amplitude (4) and vertex functions (6) contain relative momenta p and q in exact form. In order to take into account relativistic corrections of the second order in p and q, the expansion is performed for all inverse denominators of the quark and gluon propagators:

$$\frac{1}{(p_{1,2} + q_{1,2})^2} = \frac{1}{Z_0}\left[1 \mp \frac{2(\eta_{1,2}pQ + \rho_{1,2}qP)}{Z_0} - \frac{p^2 + 2pq + q^2}{Z_0} + \cdots\right],$$

$$\frac{1}{(p_1 + q_1 + q_2)^2 - m_b^2} = \frac{1}{Z_1}\left[1 - \frac{2pQ + p^2}{Z_1} + \frac{4(pQ)^2}{Z_1^2} + \cdots\right],$$

$$\frac{1}{(k_2 - q_1)^2 - m_c^2} = \frac{1}{Z_2}\left[1 + \frac{2k_2 q - q^2}{Z_2} + \frac{4(k_2 q)^2}{Z_2^2} + \cdots\right], \tag{14}$$

where $s = (k_1 + k_2)^2 = (P + Q)^2 = x_1 x_2 S$ and $t = (P - k_1)^2 = (Q - k_2)^2$ are the Mandelstam variables for the gluonic subprocess, and the leading-order expansion denominators are $Z_0 = s\eta_{1,2}\rho_{1,2} + (\eta_{1,2} - \rho_{1,2})(\eta_{1,2}M_{bc}^2 - \rho_{1,2}M_{\bar{b}\bar{c}}^2)$, $Z_1 = s\eta_1 - \eta_2(\eta_1 M_{bc}^2 - M_{\bar{b}\bar{c}}^2) - m_b^2$, and $Z_2 = t\rho_1 - \rho_1\rho_2 M_{\bar{b}\bar{c}}^2 - m_c^2$. The amplitude (4) contains 16 different denominators to be expanded in the manner of Eq. (14). Temporarily neglecting the bound-state corrections, it can be found that expansion denominators have one of the following forms: $s\eta_{1,2}$, $s\eta_{1,2}^2$, $\eta_{1,2}(M^2 - t)$, or $\eta_{1,2}(M^2 - s - t)$. Then, taking into account kinematical restrictions for s and t, along with the nonrelativistic estimate $\eta_1 = \rho_1 = m_c/(m_c + m_b) \approx 1/4$ for (bc) diquarks, one can conclude that the expansion parameters in (14) are at least as small as $4p^2/M^2$ and $4q^2/M^2$. Preserving in the expanded amplitude terms up to the second order in both of the relative momenta p and q, the angular integration can be performed according to the relations for S-wave states:

$$\int \frac{\Psi_0(\mathbf{p})}{\sqrt{\frac{e_c(p)}{m_c}\frac{e_c(p) + m_c}{2m_c}\frac{e_b(p)}{m_b}\frac{e_b(p) + m_b}{2m_b}}}\frac{d\mathbf{p}}{(2\pi)^3}$$

$$= \frac{1}{\sqrt{2\pi}}\int_0^\infty \frac{p^2 R_p(p)}{\sqrt{\frac{e_c(p)}{m_c}\frac{e_c(p) + m_c}{2m_c}\frac{e_b(p)}{m_b}\frac{e_b(p) + m_b}{2m_b}}}\,dp,$$

$$\int \frac{p_\mu p_\nu \Psi_0(\mathbf{p})}{\sqrt{\frac{e_c(p)}{m_c}\frac{e_c(p) + m_c}{2m_c}\frac{e_b(p)}{m_b}\frac{e_b(p) + m_b}{2m_b}}}\frac{d\mathbf{p}}{(2\pi)^3}$$

$$= -\frac{g_{\mu\nu} - v_{1\mu}v_{1\nu}}{3\sqrt{2\pi}}\int_0^\infty \frac{p^4 R_p(p)}{\sqrt{\frac{e_c(p)}{m_c}\frac{e_c(p) + m_c}{2m_c}\frac{e_b(p)}{m_b}\frac{e_b(p) + m_b}{2m_b}}}\,dp, \tag{15}$$

where $R_p(p)$ is the radial wave function in the momentum representation.

In order to calculate the cross section, the squared modulus of the amplitude has to be summed upon the

final polarizations in the case of axial-vector diquarks, and also has to be averaged over polarizations of the initial gluons using the following relations:

$$\sum_\lambda \varepsilon_{P,Q}^\mu \varepsilon_{P,Q}^{*\ \nu} = v_{1,2}^\mu v_{1,2}^\nu - g^{\mu\nu},$$

$$\sum_\lambda \varepsilon_{1,2}^\mu \varepsilon_{1,2}^{*\ \nu} = \frac{k_1^\mu k_2^\nu + k_1^\nu k_2^\mu}{(k_1 k_2)} - g^{\mu\nu}. \tag{16}$$

Then it is also averaged over 8×8 possible initial gluon color states and summed over diquark color indices A and B:

$$e^{c_1 c_2 A} e^{c_3 c_4 A} = \delta^{c_1 c_3} \delta^{c_2 c_4} - \delta^{c_1 c_4} \delta^{c_2 c_3},$$

$$d^{c_1 c_2 A} d^{c_3 c_4 A} = \delta^{c_1 c_3} \delta^{c_2 c_4} + \delta^{c_1 c_4} \delta^{c_2 c_3}. \tag{17}$$

In the case of the diquark pair with identical spin states and masses, the cross section can be presented as

$$d\sigma[gg \to D_{bc} + \bar{D}_{\bar{b}\bar{c}}](s,t) = \frac{\pi M_{bc} M_{\bar{b}\bar{c}} \alpha_s^4}{65536 s^2} |R(0)|^4 [F^{(1)}(s,t) - 3(2\omega_{01} + 2\omega_{10} - \omega_{11})F^{(1)}(s,t)$$
$$+ \frac{27}{2}(\omega_{01} + \omega_{10})^2 F^{(1)}(s,t) + \frac{1}{2}\omega_{\frac{11}{22}}(2 - 9\omega_{01} - 9\omega_{10})F^{(2)}(s,t) + \omega_{\frac{11}{22}}^2 F^{(3)}(s,t)], \tag{18}$$

while for the final state containing particles of unequal masses it has a more complicated form:

$$d\sigma[gg \to S(AV)D_{bc} + AV(S)\bar{D}_{\bar{b}\bar{c}}](s,t)$$
$$= \frac{\pi M_{bc} M_{\bar{b}\bar{c}} \alpha_s^4}{65536 s^2} |R_{SD_{bc}}(0)|^2 |R_{AV\bar{D}_{\bar{b}\bar{c}}}(0)|^2 \times \left[F^{(1)}(s,t) - 3\left(\omega_{01}^S + \omega_{10}^S + \omega_{01}^{AV} + \omega_{10}^{AV} - \frac{1}{2}\omega_{11}^S - \frac{1}{2}\omega_{11}^{AV}\right)F^{(1)}(s,t) \right.$$
$$+ 9(\omega_{01}^S + \omega_{10}^S)(\omega_{01}^{AV} + \omega_{10}^{AV}) \times F^{(1)}(s,t) + \frac{9}{4}(\omega_{01}^S + \omega_{10}^S)^2 F^{(1)}(s,t) + \frac{9}{4}(\omega_{01}^{AV} + \omega_{10}^{AV})^2 F^{(1)}(s,t)$$
$$+ \frac{1}{4}\omega_{\frac{11}{22}}^S(2 - 3\omega_{01}^S - 3\omega_{10}^S - 6\omega_{01}^{AV} - 6\omega_{10}^{AV})F^{(2)}(s,t) + \frac{1}{4}\omega_{\frac{11}{22}}^{AV}(2 - 3\omega_{01}^{AV} - 3\omega_{10}^{AV} - 6\omega_{01}^S - 6\omega_{10}^S)F^{(2)}(s,t)$$
$$\left. + \omega_{\frac{11}{22}}^S \omega_{\frac{11}{22}}^{AV} F^{(3)}(s,t) + \frac{1}{4}(\omega_{\frac{11}{22}}^S + \omega_{\frac{11}{22}}^{AV})^2 F^{(4)}(s,t) \right]. \tag{19}$$

The relativistic parameters ω_{nk} are expressed through momentum integrals of the double heavy diquark radial wave function $R_p(p)$:

$$I_{nk} = \int_0^{m_c} p^2 R_p(p) \sqrt{\frac{(e_c(p) + m_c)(e_b(p) + m_b)}{2e_c(p) 2e_b(p)}}$$
$$\times \left(\frac{e_c(p) - m_c}{e_c(p) + m_c}\right)^n \left(\frac{e_b(p) - m_b}{e_b(p) + m_b}\right)^k dp,$$

$$\omega_{nk} = \sqrt{\frac{2}{\pi}} \frac{I_{nk}}{R(0)}, \tag{20}$$

and

$$R(0) = \sqrt{\frac{2}{\pi}} \int_0^\infty p^2 R_p(p) dp \tag{21}$$

is the value of the coordinate wave function at the origin. The first term in Eqs. (18) and (19) is proportional to the single function $F^{(1)}(s,t)$ and corresponds to the zeroth-order result in heavy quark velocity expansion of the cross sections, and the other terms containing products of the

form $\omega_{nk}F^{(i)}(s,t)$ represent relativistic corrections to it. The analytical results for the functions $F^{(i)}(s,t)$ are too lengthy and cannot be given here in an explicit form, but they are provided as Supplemental Material [31] to the electronic version of this paper.

III. NUMERICAL RESULTS AND DISCUSSION

The quasipotential wave functions of the double heavy diquarks in the (anti)triplet color state are obtained by numerical solving of the Schrödinger equation with an effective relativistic Hamiltonian based on the QCD generalization of the Breit potential, which was additionally improved by the scalar and vector exchange confinement terms, as is described in detail in Ref. [21]. The values of diquark masses and relativistic parameters defined by Eq. (20) are given in Table I. There is no such model available for sextuplet diquarks, so all their nonperturbative parameters, including $R(0)$, are simply taken to be equal to those of triplet diquarks, which is the common practice allowing us to roughly estimate the order of contributions from these color states [5,19,23–28]. The relativistic parameters ω_{nk} from Table I are almost indistinguishable for scalar and axial-vector (*bc*) diquarks, and this fact was

TABLE I. Numerical values of the parameters describing scalar and axial-vector (bc) diquarks.

Diquark state	$n^{2S+1}L_J$	$M,$ GeV	$R^{\text{NR}}(0)$ GeV$^{3/2}$	$R(0),$ GeV$^{3/2}$	ω_{10}	ω_{01}	$\omega_{\frac{11}{22}}$	ω_{11}
SD_{bc}	1^1S_0	6.517	0.67	0.54	0.0383	0.0045	0.0131	0.000 39
AVD_{bc}	1^3S_1	6.526	0.67	0.52	0.0384	0.0045	0.0132	0.000 38

used to slightly simplify the final view of the cross section (19). The definition (20) of the relativistic integrals I_{nk} contains a cutoff at the value of c-quark mass $\Lambda = m_c$. Although the integrals (20) are numerically convergent, the relativistic wave function cannot be reliably calculated in the region $p \gtrsim m_c$ in the considered model. It should also be noted that the formulation of the effective relativistic Hamiltonian in Ref. [21] assumes expansion of the interaction potential in powers of $|p|/\frac{2m_c m_b}{m_b+m_c} \approx \frac{2}{3}|p|/m_c$, and the expansion parameters of Eq. (14) were estimated as $\sim \frac{1}{4}|p|^2/m_c^2$. So, the current choice of cutoff for relativistic terms preserves the validity of both relativistic expansions and also prevents the contribution of large numerical errors connected with multiplication of the wave function by additional p^2 factors in the highly relativistic region. There is no such numerical instability involved in calculation of the parameter $R(0)$ determining the zeroth-order contribution in v, which is therefore defined over the whole available momentum range in both nonrelativistic and relativistic approximations. The nonrelativistic version of this parameter $R^{\text{NR}}(0)$ has the same formal definition $R^{\text{NR}}(0) = \sqrt{2/\pi} \int p^2 R_p^{\text{NR}}(p)dp$, with the only difference being that it is calculated with the simple Cornell potential model $V^{\text{NR}}(r) = -2\alpha_s/(3r) + 1/2(Ar + B)$ in contrast to the complicated Breit-based Hamiltonian used to obtain $R(0)$. Therefore, the parameter $R(0)$ purely reflects the nonperturbative relativistic effects of quark-quark

interaction within the bound state, while all auxiliary normalization factors of the wave function transformation law (5) have been incorporated into the correction terms $\omega_{nk}F^{(i)}(s,t)$ in Eqs. (18) and (19).

The numerical results for the total cross section of pair scalar and axial-vector (bc) diquark production corresponding to the LHC energies $\sqrt{S} = 7$ and 14 TeV are presented in Table II. The integration in (1) was performed with the partonic distribution functions CTEQ5L and CTEQ6L1 [37]. Both renormalization and factorization scales were set to $\mu = \sqrt{(M_{bc} + M_{\bar{b}\bar{c}})^2/4 + P_T^2}$, where P_T is the transverse momentum of the final diquarks, and the leading-order result for the strong coupling with the initial condition $\alpha_s(M_Z) = 0.118$ was used. In the nonrelativistic limit, all parameters ω_{nk} are taken to equal zero, so that only the $F^{(1)}(s,t)$ term survives in the square brackets of Eq. (18), and diquark masses are assumed to be equal to the sums of their constituent (anti)quark masses $M_0 = m_b + m_c$. The cross sections calculated in such approximation are marked as σ_{nonrel} in Table II. As shown in Table I, the nonrelativistic parameter $R^{\text{NR}}(0)$ has the value $R^{\text{NR}}(0) = 0.67$ GeV$^{3/2}$ for (bc) diquarks in the considered model [21,22], lying close to the result 0.73 GeV$^{3/2}$ from Ref. [38].

Table II contains numerical results for all ten independent spin (scalar and axial-vector) and color (triplet and sextuplet) state combinations of the final diquarks

TABLE II. Cross sections of the pair (bc) diquark production in proton-proton collisions (nb). The results in nonrelativistic approximation (*nonrel.*) and with relativistic effects (*rel.*) are given.

	$\sqrt{S} = 7$ TeV				$\sqrt{S} = 14$ TeV			
	CTEQ5L		CTEQ6L1		CTEQ5L		CTEQ6L1	
Diquark pair	σ_{nonrel}	σ_{rel}	σ_{nonrel}	σ_{rel}	σ_{nonrel}	σ_{rel}	σ_{nonrel}	σ_{rel}
$S(bc)_{\bar{3}} + S(\bar{b}\bar{c})_3$	0.063	0.023	0.057	0.021	0.14	0.05	0.12	0.043
$S(bc)_{\bar{3}} + S(\bar{b}\bar{c})_{\bar{6}}$	0.007	0.003	0.007	0.003	0.016	0.006	0.014	0.005
$S(bc)_6 + S(\bar{b}\bar{c})_{\bar{6}}$	0.04	0.015	0.037	0.013	0.088	0.032	0.078	0.029
$AV(bc)_{\bar{3}} + AV(\bar{b}\bar{c})_3$	0.25	0.068	0.23	0.062	0.55	0.15	0.48	0.13
$AV(bc)_{\bar{3}} + AV(\bar{b}\bar{c})_{\bar{6}}$	0.29	0.076	0.27	0.07	0.63	0.17	0.56	0.15
$AV(bc)_6 + AV(\bar{b}\bar{c})_{\bar{6}}$	1.4	0.38	1.3	0.35	3.1	0.84	2.7	0.74
$S(bc)_{\bar{3}} + AV(\bar{b}\bar{c})_3$	0.031	0.009	0.029	0.009	0.069	0.02	0.061	0.018
$S(bc)_{\bar{3}} + AV(\bar{b}\bar{c})_{\bar{6}}$	0.17	0.051	0.15	0.047	0.37	0.11	0.32	0.098
$S(bc)_6 + AV(\bar{b}\bar{c})_3$	0.16	0.047	0.14	0.043	0.34	0.1	0.3	0.091
$S(bc)_6 + AV(\bar{b}\bar{c})_{\bar{6}}$	0.14	0.041	0.12	0.037	0.3	0.089	0.26	0.078

contributing to $\sigma[pp \to D_{bc} + \bar{D}_{\bar{b}\bar{c}} + X]$. The other six cross sections can be obtained by interchanging with simultaneous charge conjugation of the diquark pair, so that $\sigma[S(bc)_6 + S(\bar{b}\bar{c})_{\bar{3}}] = \sigma[S(bc)_{\bar{3}} + S(\bar{b}\bar{c})_{\bar{6}}]$, $\sigma[AV(bc)_6 + S(\bar{b}\bar{c})_{\bar{3}}] = \sigma[S(bc)_{\bar{3}} + AV(\bar{b}\bar{c})_{\bar{6}}]$, and so on. Formally, in the case of a final diquark pair with unequal spin states, the diquark masses have to be interchanged too, but due to their very close proximity in the actual cases of scalar and axial-vector diquarks ($M_{S(bc)} = 6.517$ GeV and $M_{AV(bc)} = 6.526$ GeV), the numerical effects on the cross section will be negligible. Table II clearly shows that gluonic fusion subprocesses involving one or two final diquarks in a(n anti)sextuplet color state provide considerable contributions, which basically prove to significantly exceed the corresponding triplet-antitriplet results. The largest contribution comes from the process of double axial-vector production, where the cross section of the $6 + \bar{6}$ pair is more than 5 times larger than its $\bar{3} + 3$ counterpart, and the cross sections for the two other possibilities $\bar{3} + \bar{6}$ and $6 + 3$ are both higher by almost 20% in comparison with $\sigma[AV(bc)_{\bar{3}} + AV(\bar{b}\bar{c})_3]$. The sextuplet contributions are also important for $S + AV$ and $AV + S$ diquark spin pairs, with all three additional subprocesses enhancing the purely triplet result by a factor of 4.5–5.5 each. Then, the simultaneous scalar

and axial-vector diquark production acquires the same order of magnitude as the main $AV + AV$ channel, in spite of $\sigma[S(bc)_{\bar{3}} + AV(\bar{b}\bar{c})_3]$ having the smallest value between all triplet-antitriplet states. The scalar-scalar diquark pair appears to be of the least significance, since its exclusively sextuplet case $6 + \bar{6}$ has only 60% of the double triplet $\bar{3} + 3$ cross section, and both cases of mixed color combinations are even more suppressed by a factor of 9. So, the $S + S$ diquark contributions to the pair double heavy baryon production are expected to be negligible. The stated relations between the various subprocesses of $gg \to D_{bc} + \bar{D}_{\bar{b}\bar{c}}$ are independent of the choice of partonic functions $f_{g/p}(x)$ or collision energy $\sqrt{S}$, and they also remain valid with relativistic corrections taken into account. Moreover, they demonstrate a remarkable stability through almost the whole range of (bc) diquark rapidity y for the corresponding differential cross section $d\sigma/dy$, as shown in Fig. 3. The invariant mass distributions presented in Fig. 4 have almost the same asymptotics at large values of $\sqrt{s}$, with the sole exception of $\bar{3} + \bar{6}$ cross sections in $S + S$ and $AV + AV$ cases, which are suppressed by 1 additional power of $s^{-1/2}$ in comparison with the sextet-antisextet and antitriplet-triplet color pairs.

The cross section of pair diquark production in proton-proton interaction $\sigma[pp \to D_{bc} + \bar{D}_{\bar{b}\bar{c}} + X]$ gives an upper
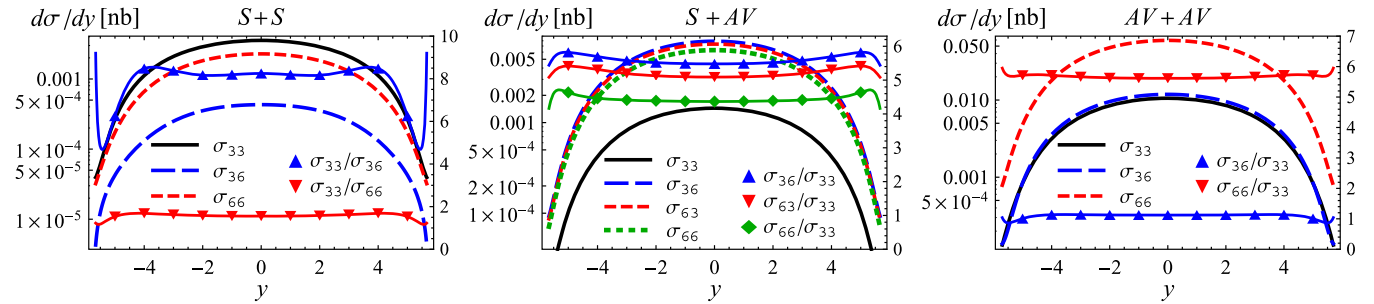

FIG. 3. The rapidity $y \equiv y_{D_{bc}}$ distributions for $S + S$ (left), $S + AV$ (center), and $AV + AV$ (right) pair double heavy diquark production at pp collision energy $\sqrt{S} = 7$ TeV. The scale at the right edge of the figures corresponds to the ratios of cross sections. The compact notations $\sigma_{33} = d\sigma[(bc)_{\bar{3}} + (\bar{b}\bar{c})_3]/dy$ and so on are used in the figures.
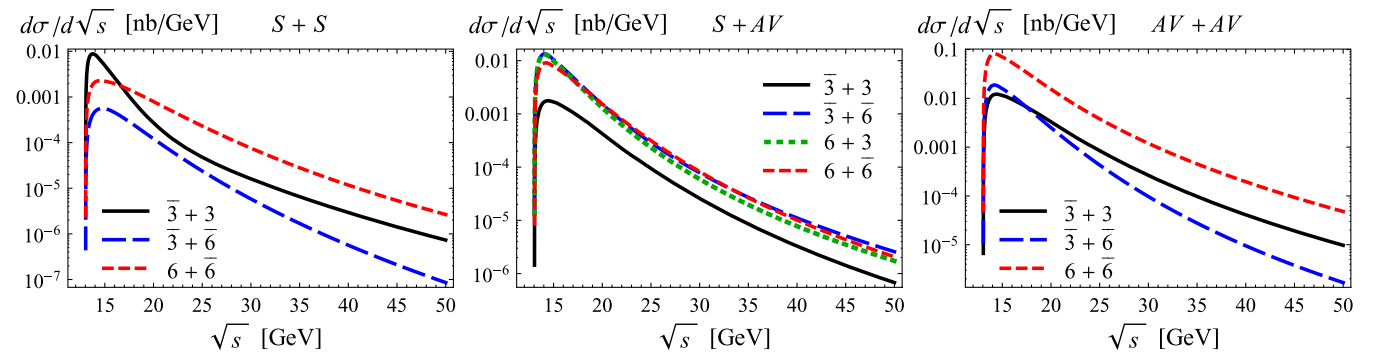

FIG. 4. The invariant mass $\sqrt{s}$ distributions for $S + S$ (left), $S + AV$ (center), and $AV + AV$ (right) pair double heavy diquark production at the energy $\sqrt{S} = 7$ TeV.

bound for the yield of the double heavy baryon pairs $(bcl_1) + (\bar{b}\bar{c}\bar{l}_2)$ in the same process summed over spin states of both baryons and also over all possible flavors of light quarks and antiquarks $l_{1,2} = u$, d, s. Adding up the contributions from Table II for the collision energy $\sqrt{S} = 7(14)$ TeV and CTEQ5L functions, we obtain the estimates 3.3(7.3) nb and 0.9(2.1) nb in nonrelativistic and relativistic cases, respectively, where the purely sextuplet channel is responsible for slightly more than half of the result [1.7 (3.8) nb and 0.5(1.1) nb], final states with mixed colors $\bar{3} + \bar{6}$ and $6 + 3$ contribute about 37% of the cross section [1.2(2.7) nb and 0.3(0.8) nb], and the 12% residue [0.4 (0.8) nb and 0.1(0.2) nb] originates from the conventional

triplet-antitriplet diquark pairs. So, under the assumption that both triplet and sextuplet states are described by the same value of $|R(0)|^2$, the processes involving one or two final sextuplets are the dominant ones for pair double heavy diquark and baryon production, and they will still prevail over the triplet-only cases even if the values of their nonperturbative parameters corresponding to $|R(0)|^2$ are found to be overestimated as much as 3–4 times.

The cross sections (18) and (19) contain several types of relativistic corrections with the net effect of up to a factor of 4 decrease in comparison with the completely nonrelativistic analysis. Such a tremendous fall is entirely caused by the Breit-like interaction between (anti)quarks in the bound
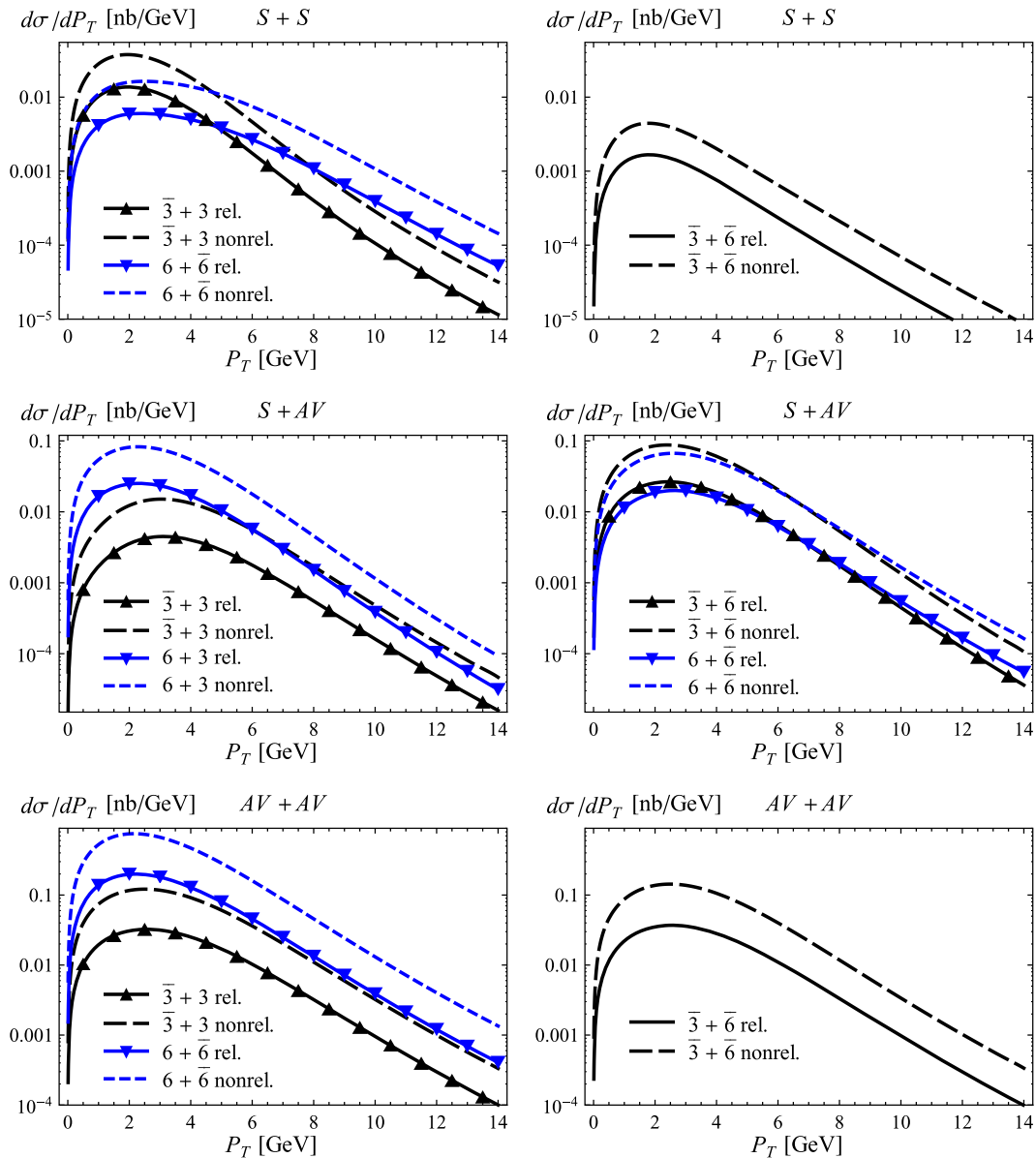

FIG. 5. The transverse momentum P_T distributions for $S + S$ (upper panel), $S + AV$ (center), and $AV + AV$ (lower panel) pair double heavy diquark production at the energy $\sqrt{S} = 14$ TeV. The results in nonrelativistic approximation (*nonrel.*) and with relativistic effects (*rel.*) are shown.

state determining the masses and wave functions of scalar and axial-vector diquarks. The transition from the non-relativistic parameter $|R^{\mathrm{NR}}(0)|^4$ to its relativistic generalization $|R_{D_{bc}}(0)|^2|R_{\bar{D}_{\bar{b}\bar{c}}}(0)|^2$ suppresses the cross section by a factor of 2.3–2.9 depending on the final spin content. Note that direct corrections to the diquark wave functions induced by relativistic terms in quark-quark interaction potential are not so large. According to Table I, the difference between $R^{\mathrm{NR}}(0)$ and $R(0)$ does not exceed 20%, but its fourth power actually entering expressions (18) and (19) significantly amplifies the decreasing effect. The diquark masses enter cross sections (18) and (19) as prefactors and also essentially influence the functions $F^{(i)}(s,t)$, so that the bound-state corrections connected with the nonzero values of bound-state energies $W_{S,AV(bc)} = M_{S,AV(bc)} - m_c - m_b \neq 0$ can be identified. These corrections also turn out to be negative and decrease the cross sections by 20%–30% against the results calculated in the nonrelativistic approximation $M_{S(bc)} = M_{AV(bc)} = m_b + m_c$. Finally, our analysis includes perturbative corrections of the second order in the (anti)quarks' relative momenta p and q [or, alternatively, $\mathcal{O}(v^2)$ order in relative velocity v], which are directly determined by the relativistic structure of the production amplitude (4). As was mentioned earlier, such corrections are represented by the terms $\omega_{nk}F^{(i)}(s,t)$ in Eqs. (18) and (19). They generally add 8%–12% to all of the considered production channels, with the exception of the following three color-spin combinations of the final diquark pair: $S_{\bar{3}} + S_{\bar{6}}$ (25%), $AV_{\bar{3}} + AV_3$ (5%), and $AV_6 + AV_{\bar{6}}$ (1.5%). The above example of a scalar-scalar pair shows that perturbative corrections can give considerable enhancements, which are, however, negligible in this particular case due to the low numerical importance of the $gg \to S(bc)_{\bar{3}} + S(\bar{b}\bar{c})_6$ subprocess. On average, $\mathcal{O}(v^2)$ corrections contribute slightly more than 6% to the upper estimate of 0.9(2.1) nb for the cross section of double heavy baryons at $\sqrt{S} = 7(14)$ TeV. The relativistic corrections do not change the visible shape of all examined cross section distributions, as shown in Fig. 5 in the example of transverse momentum distribution $d\sigma/dP_T$.

The total error of the numerical results for cross sections (18) and (19) presented in Table II is basically given by the main sources of relativistic corrections and can be estimated as 44%. The 10% uncertainty of wave functions calculated in the potential model is responsible for the main 40% error coming from the fourth power of $R(0)$ [21]. The perturbative contributions from the fourth and higher orders of the amplitude expansion can be taken to be 10%, since the calculated second-order corrections are already small. Another 15% error source is introduced by the uncertainty of the CTEQ5L and CTEQ6L1 partonic distribution functions [37,39]. In order to obtain the final value of 44%, all mentioned uncertainties are summed in quadrature.

In this paper, a complete study of pair (bc) diquark production at the LHC center-of-mass energies $\sqrt{S} = 7$ and 14 TeV has been performed in the leading order of the gluonic fusion channel. Several types of relativistic improvements to the cross section have been implemented according to the framework of the relativistic quark model. The corresponding nonperturbative parameters calculated in the assumption of a Breit-like interaction between (anti)quarks of the bound state are found to significantly decrease the cross section in comparison to the estimates based on the completely nonrelativistic Cornell model. The perturbative $\mathcal{O}(v^2)$ corrections originating from the production amplitude expansions can give moderate improvements, although they turn out to be irrelevant for the main subprocess $gg \to AV(bc)_6 + AV(\bar{b}\bar{c})_{\bar{6}}$ determining almost half of the final result. The total error of the calculation is estimated to be on the level of 50%, which is mostly determined by the accuracy of the double heavy diquark wave functions obtained in the considered model. It is shown that sextuplet color states of the final diquarks appear to dominate the total cross section. So, pair double heavy baryon production can represent a good test for the color-sextuplet production mechanism.

APPENDIX: THE STRUCTURE OF SUPPLEMENTAL MATERIAL

The electronic Supplemental Material [31] to the paper consists of 84 textual files containing the explicit form of the functions $F^{(i)}(s,t)$ entering the cross sections (18) and (19) for all ten independent spin- and color-state combinations of the final diquark pair. The functions are linearly expanded in diquark bound energies $W_{bc} = M_{bc} - m_c - m_b$ and $W_{\bar{b}\bar{c}} = M_{\bar{b}\bar{c}} - m_c - m_b$:

$$F^{(i)}(s,t) = F_0^{(i)}(s,t) + W_{bc}F_1^{(i)}(s,t) + W_{\bar{b}\bar{c}}F_2^{(i)}(s,t),$$

(A1)

where the last term exists only for the $S + AV$ final states with two diquarks of unequal masses. Then, for example, the file F[3S + 6AV](1).0 contains the function $F_0^{(1)}(s,t)$ of the $S(bc)_{\bar{3}} + AV(\bar{b}\bar{c})_{\bar{6}}$ pair.

[1] M. Mattson *et al.* (SELEX Collaboration), Phys. Rev. Lett. **89,** 112001 (2002); J. O. Ojo, R. O. Osoniyi, and A. O. Aboderin (SELEX Collaboration), Czech. J. Phys. **53,** B201 (2003); A. Ocherashvili *et al.* (SELEX Collaboration), Phys. Lett. B **628,** 18 (2005).

[2] R. Chistov *et al.* (Belle Collaboration), Phys. Rev. Lett. **97,** 162001 (2006); B. Aubert *et al.* (*BABAR* Collaboration), Phys. Rev. D **74,** 011103 (2006); R. Aaij *et al.* (LHCb Collaboration), J. High Energy Phys. 12 (2013) 090; Y. Kato *et al.* (Belle Collaboration), Phys. Rev. D **89,** 052003 (2014).

[3] V. V. Kiselev and A. K. Likhoded, Phys. Usp. **45,** 455 (2002); arXiv:hep-ph/0208231.

[4] N. Brambilla, A. Vairo, and T. Roesch, Phys. Rev. D **72,** 034021 (2005).

[5] C. H. Chang, C. F. Qiao, J. X. Wang, and X. G. Wu, Phys. Rev. D **73,** 094022 (2006).

[6] C. Albertus, E. Hernandez, J. Nieves, and J. M. Verde-Velasco, Eur. Phys. J. A **31,** 691 (2007); **32,** 183 (2007); **36,** 119 (2008).

[7] C. H. Chang, J. X. Wang, and X. G. Wu, Comput. Phys. Commun. **177,** 467 (2007); **181,** 1144 (2010).

[8] M. Karliner and J. L. Rosner, Phys. Rev. D **90,** 094007 (2014).

[9] H. Y. Cheng, Front. Phys. **10,** 101406 (2015).

[10] M. Karliner, Int. J. Mod. Phys. A **30,** 1530007 (2015); EPJ Web Conf. **96,** 01019 (2015).

[11] X. C. Zheng, C. H. Chang, and Z. Pan, Phys. Rev. D **93,** 034019 (2016).

[12] S. Fleck, B. Silvestre-Brac, and J. M. Richard, Phys. Rev. D **38,** 1519 (1988).

[13] A. F. Falk, M. Luke, M. J. Savage, and M. B. Wise, Phys. Rev. D **49,** 555 (1994); M. Anselmino, E. Predazzi, S. Ekelin, S. Fredriksson, and D. Lichtenberg, Rev. Mod. Phys. **65,** 1199 (1993); A. V. Berezhnoy, V. V. Kiselev, and A. K. Likhoded, Phys. At. Nucl. **59,** 870 (1996).

[14] G. T. Bodwin, E. Braaten, and G. P. Lepage, Phys. Rev. D **51,** 1125 (1995); **55,** 5853 (1997).

[15] M. Neubert, Phys. Rep. **245,** 259 (1994).

[16] D. Ebert, R. N. Faustov, V. O. Galkin, and W. Lucha, Phys. Rev. D **76,** 114015 (2007); W. Chen, T. G. Steele, and S. L. Zhu, Universe **2,** 13 (2014); arXiv:1403.7457.

[17] N. Brambilla *et al.* Eur. Phys. J. C **71,** 1534 (2011); **74,** 2981 (2014); G. T. Bodwin, E. Braaten, E. Eichten, S. L. Olsen, T. K. Pedlar, and J. Russ, arXiv:1307.7425.

[18] V. V. Kiselev, Phys. Rev. D **58,** 054008 (1998); V. V. Kiselev and A. E. Kovalsky, Phys. At. Nucl. **63,** 1640 (2000); D. A. Gunter and V. A. Saleev, *Proceedings of the 16th International Workshop, QFTHEP2001,* 264 (2001); A. P. Martynenko, Phys. At. Nucl. **70,** 1305 (2007).

[19] G. Chen, X. G. Wu, Z. Sun, Y. Ma, and H. B. Fu, J. High Energy Phys. 12 (2014) 018.

[20] V. V. Braguta, V. V. Kiselev, and A. E. Chalov, Phys. At. Nucl. **65,** 1537 (2002).

[21] A. P. Martynenko and A. M. Trunin, Phys. Rev. D **89,** 014004 (2014).

[22] A. P. Martynenko and A. M. Trunin, Eur. Phys. J. C **75,** 138 (2015).

[23] J. P. Ma and Z. G. Si, Phys. Lett. B **568,** 135 (2003).

[24] C. H. Chang, J. P. Ma, C. F. Qiao, and X. G. Wu, J. Phys. G **34,** 845 (2007).

[25] J. W. Zhang, X. G. Wu, T. Zhong, Y. Yu, and Z. Y. Fang, Phys. Rev. D **83,** 034026 (2011).

[26] J. Jiang, X. G. Wu, Q. L. Liao, X. C. Zheng, and Z. Y. Fang, Phys. Rev. D **86,** 054021 (2012).

[27] J. Jiang, X. G. Wu, S. M. Wang, J. W. Zhang, and Z. Y. Fang, Phys. Rev. D **87,** 054027 (2013).

[28] G. Chen, X. G. Wu, J. W. Zhang, H. Y. Han, and H. B. Fu, Phys. Rev. D **89,** 074020 (2014).

[29] V. A. Matveev, V. I. Savrin, A. N. Sissakian, and A. N. Tavkhelidze, Theor. Math. Phys. **132,** 1119 (2002).

[30] D. Ebert and A. P. Martynenko, Phys. Rev. D **74,** 054008 (2006); D. Ebert, R. N. Faustov, V. O. Galkin, and A. P. Martynenko, Phys. Lett. B **672,** 264 (2009).

[31] See Supplemental Material at http://link.aps.org/supplemental/10.1103/PhysRevD.93.114029 for zip-archive.

[32] V. V. Kiselev, A. K. Likhoded, S. R. Slabospitsky, and A. V. Tkabladze, Sov. J. Nucl. Phys. **49,** 1041 (1989).

[33] J. Kublbeck, M. Böhm, and A. Denner, Comput. Phys. Commun. **60,** 165 (1990); T. Hahn, Comput. Phys. Commun. **140,** 418 (2001).

[34] J. A. M. Vermaseren, arXiv:math-ph/0010025.

[35] S. J. Brodsky and J. R. Primack, Ann. Phys. (N.Y.) **52,** 315 (1969).

[36] R. N. Faustov, Ann. Phys. (N.Y.) **78,** 176 (1973).

[37] H. L. Lai, J. Huston, S. Kuhlmann, J. Morfin, F. Olness, J. F. Owens, J. Pumplin, and W. K. Tung, Eur. Phys. J. C **12,** 375 (2000); J. Pumplin, D. R. Stump, J. Huston, H.-L. Lai, P. Nadolsky, and W.-K. Tung, J. High Energy Phys. 07 (2002) 012.

[38] S. S. Gershtein, V. V. Kiselev, A. K. Likhoded, and A. I. Onishchenko, Phys. Rev. D **62,** 054021 (2000).

[39] A. P. Martynenko and A. M. Trunin, Phys. Lett. B **723,** 132 (2013).